

Overcoming the Limitations of Layer Synchronization in Spiking Neural Networks

Roel Koopman
imec

Amirreza Yousefzadeh
University of Twente

Mahyar Shahsavari
Radboud University

Guangzhi Tang
Maastricht University

Manolis Sifalakis
imec

Abstract

Currently, neural-network processing in machine learning applications relies on layer synchronization, whereby neurons in a layer aggregate incoming currents from all neurons in the preceding layer, before evaluating their activation function. This is practiced even in artificial Spiking Neural Networks (SNNs), which are touted as consistent with neurobiology, in spite of processing in the brain being, in fact asynchronous. A truly asynchronous system however would allow all neurons to evaluate concurrently their threshold and emit spikes upon receiving any presynaptic current.

Omitting layer synchronization is potentially beneficial, for latency and energy efficiency, but asynchronous execution of models previously trained with layer synchronization may entail a mismatch in network dynamics and performance.

We present a study that documents and quantifies this problem in three datasets on our simulation environment that implements *network asynchrony*, and we show that models trained with layer synchronization either perform sub-optimally in absence of the synchronization, or they will fail to benefit from any energy and latency reduction, when such a mechanism is in place.

We then “make ends meet” and address the problem with *unlayered backprop*, a novel backpropagation-based training method, for learning models suitable for asynchronous processing. We train with it models that use different neuron execution scheduling strategies, and we show that although their neurons are more reactive, these models consistently exhibit lower overall spike density (up to 50%), reach a correct decision faster (up to 2x) without integrating all spikes, and achieve superior accuracy (up to ~10% higher). Our findings suggest that asynchronous event-based (neuromorphic) AI computing is indeed more efficient, but we need to seriously rethink how we train our SNN models, to benefit from it.

1 Introduction

Artificial Neural Networks (ANNs) are the foundation behind many of the recently successful developments in AI, such as in computer vision [54, 58] and natural language processing [57, 5]. To match the complexity of the ever more demanding tasks, networks have grown in size, with advanced large language models having billions of parameters [65]. With this the power consumption exploded [28], limiting the deployment to large data centers. In an effort to learn from our brain’s superior power efficiency, and motivated in neuroscience research, SNNs [30] bolster as an alternative. They use discrete binary or graded spikes (events) for communication, are suited for processing sparse features [18], and when combined with asynchronous event-based processing are assumed to enhance latency and energy efficiency (and scalability). Sparsity leads to fewer synaptic operations, resulting in low energy consumption, and asynchronous operation potentiates concurrent evaluation of all neurons in the network purely event-driven, leading to low latency.

Conventional highly parallel ANN compute accelerators, such as Graphics Processing Units (GPUs) and Tensor Processing Units (TPUs), which are primarily optimized for dense vectorized matrix operations, face inherent challenges in exploiting sparsity for improving their energy efficiency. Targeting the commonplace practiced way of executing ANNs layer-after-layer has left them with poor support for asynchronous processing too (for improving latency). At best, they parallelize processing within a layer and/or pipeline processing across layers. This leaves an exploration space for neuromorphic processors that try to excel in handling the event-driven nature of SNNs and leverage asynchronous concurrent processing, offering efficiency advantages in various tasks [19, 21, 36].

However, despite this advancement, the training of SNNs today very often conveniently relies on conventional end-to-end ANN training methods for performance [9], which organize/synchronize computations per-layer rather than event-driven per neuron [17]. Specifically, at any given discrete timestep within a neuron layer, first, the total of all presynaptic currents (from the preceding layer) must be computed and integrated, before postsynaptic neurons in the current layer update their state and evaluate their activation function (i.e. emitting new spikes). For consistency, neuron evaluation in one layer must thus complete and synchronize before proceeding to evaluate neurons of a next layer. This *breadth-first* processing approach (with per layer synchronization), while it facilitates use of vectorized computing hardware (such as GPUs) during training, it introduces dependencies on synchronization that could impact model accuracy if altered during inference. Consequently, even asynchronous neuromorphic processors, such as Loihi [10], have integrated mechanisms to ensure (and enforce) layer synchronization.

This leaves a crucial (efficiency) aspect of SNNs relatively unexplored: the ability to allow spiking completely asynchronously across the network without having separate phases for integration and firing, just like in our brain [63]. In that neurophysical modus operandi, neurons can fire and receive currents anywhere in the network at any time, completely independent, a concept we term "*network asynchrony*". Allowing network asynchrony can be advantageous [42], as we confirm in our results. Spike activity can quickly propagate deep into the network without being bound by synchronization barriers, reducing latency. Furthermore, adhering to layer synchronization could lead to increased computational overhead as the network scales, as suggested by Amdahl's law [46]. This implies that the overhead grows non-linearly by adding more computational units to a group that needs to be synchronized at some point in time [60]. With network asynchrony, such groups can be kept smaller, and the number of synchronization moments can be minimized, potentially reducing the waiting time.

In this paper, we demonstrate this problem and explore solutions. Using a simulator that implements the concept of network asynchrony, we provide quantitative results based on 3 benchmark datasets (with different spatio-temporal structures) that show the performance degradation and latency/energy inefficiency resulting from changes in model dynamics when trained with layer synchronization and later deployed for asynchronous inference. We then explore potential solutions by proposing a novel gradient (backpropagation-based) training method, that can be parameterized with various neuron execution scheduling strategies for asynchronous processing, and vectorization abilities that may be available in different neuromorphic processors. We show that using this training method, it is possible to prepare models that achieve superior accuracy and, at the same time, can save energy and inference latency under asynchronous processing (when compared to the conventional breadth-first processing in GPUs). This work opens a space with unique potential for design space explorations aimed to bridge the efficiency gap between neural network model training and asynchronous processor design.

2 Related work

The term "asynchronous processing" is often used whenever neurons can be active in parallel and communicate asynchronously, even if some synchronization protocol is enforced to control the order of spikes and synaptic current processing [44, 22, 51, 61]. Another kind of asynchrony is related to input coding[15]. In this context, synchronizing means grouping spikes (events) into frames, a topic that has extensively been researched [18, 33, 43, 45, 56]. Neither of the two, however, is the focus of this work. Here, asynchrony refers solely to activity within the network not being artificially bound by any order restriction. This has been researched for simulating biologically accurate neural networks [29, 32, 31], but remains under-explored in the context of executing SNNs for machine learning. In this context, grouping and processing in layers is just one convenient way [34].

Few event-driven neuromorphic processors, such as μ Brain [53] and Speck [6], are fully event-driven and lack any layer synchronization mechanism. This makes them notorious for training out-of-the-box with mainstream model training tools that rely on per-layer synchronization (e.g., PyTorch). Speck developers propose to train their models with hardware in-the-loop [27] to reduce the mismatch between the training algorithms and the inference hardware. However this method does not provide a general solution for training asynchronous neural networks. Others, like SpiNNaker [14] and TrueNorth [1], use timer-based synchronization, or Loihi [10] and Seneca [55] use barrier synchronization between layers, in order to warrant that the asynchronous processing dynamics on hardware are aligned at layer boundaries with models trained in software (with layer synchronization). This, however, entails an efficiency penalty, as we will show.

Functionally, the most suitable type of model for end-to-end asynchronous processing is probably rate-coded SNN models, whereby neurons can integrate state and communicate independently from any

other neuron. These models are trained like ANNs [64, 26, 11] or converted from pre-trained ANNs [47, 25]. Therefore, to be accurate under asynchronous processing, it is required to run the inference for a long time, reducing the latency and energy benefit of using SNNs [49].

Alternative to rate-coding models are temporal-coding models, with time-to-first spike (TTFS) [41, 52, 23, 7] or order encoding [4]. They are very sparse (hence energy efficient) but very cumbersome and elaborate to convert from ANNs [39, 52] or train directly [23, 7], less tolerant to noise [7], and their execution so far, while event-based, requires some form of synchronization or a reference time. Efficiency is thus only attributable to the reduced number of spikes, all of which need to be evaluated in order before a decision is reached. Other alternative encodings for event-based processing of SNNs include phase-coding [24] and burst coding [40], which are, however, no more economical than rate coding and have not been shown, to our knowledge, to attain competitive performance.

The approach presented in this paper is, in fact, unique in enabling the trainability of models for event-based asynchronous execution, providing efficiency from processing only a subset of spikes, and delivering consistent performance and tolerance to noise. Also relevant to the works in this paper are SparseProp [12] and EventProp [59] on efficient event-based simulation and training, respectively. EventProp[59] is potentially more economical than discrete-time backpropagation for training event-based models for asynchronous processing (and fully compatible with the work in this paper), but it has not been shown how its complexity scales beyond 1 hidden layer. SparseProp [12] proposes an efficient neuron execution scheduling strategy for asynchronous processing in software simulation. An effective hardware implementation of this scheduling strategy can be found in [35], which has inspired the herein proposed “*momentum schedule*”. Moreover, we advance this research by demonstrating how to train SNN models using this event scheduler.

3 Methods for simulating and training of asynchronous SNNs

In this section, we provide an overview of our methodology. We first introduce our simulator for SNN processing with network asynchrony and then show how this is used for training.

3.1 Simulating asynchronous SNNs

The SNNs used in this work consist of L layers of Leaky Integrate and Fire (LIF) neurons [18], with each layer l for $1 \leq l \leq L$ having $N^{(l)}$ neurons and being fully-connected to the next layer $l + 1$, except for the output layer. Each input feature is connected to all neurons in the first layer. Every connection has a synaptic weight. Using these weights, we can compute the incoming current x per neuron resulting from spikes, as per equation 3.

Each LIF neuron has a membrane potential exponentially decaying over time based on some membrane time constant τ_m . We use the analytical solution (see equation 4) to compute the decay. By keeping track of the membrane potential $u[t]$ and the elapsed time Δt since time t , it is possible to precisely calculate the membrane potential for $t + \Delta t$. Therefore, computations are required only when $x[t + \Delta t] > 0$.

To determine if a neuron spikes, a threshold function Θ checks if the membrane potential exceeds a threshold U_{thr} , following equation 5. If $\Theta(u) = 1$, the membrane potential is immediately hard reset to 0. Soft reset is another option in the simulator often defended in the literature [16] as well as refractoriness [48]. However for simplicity here we only experiment with hard reset.

3.1.1 Event-driven state updates

We can vectorize the computations introduced in the previous section to perform them on a per-layer basis. This is the “layered” inference approach, which implies layer synchronization, since all neurons of one layer evaluate their state at the same instant. An alternative to this is an event-driven approach, where the computations for state updates are applied in response to new spike arrivals. Spikes can be emitted at any time by any neuron, affecting the states of postsynaptic neurons independently of others. Such an approach can achieve a true representation of network asynchrony.

When using event-driven updates, the network dynamics evolve with each spike. A single spike can generate multiple currents, each linked to a specific time t , determined by the initiating input activity. Let K_t represent the atomic computational unit that is executed for an input current received at time t and that will update the state of a single neuron and evaluate its threshold function (activation). The exact computations for a LIF neuron can be found in section A.2. The order in which K_t is executed across neurons inside the entire network (and not just in one layer) affects the output of the network due

to the non-linear nature of K_t (see figure 1 for an example of the effect this can have). For simplicity, it is assumed that the currents resulting from the same spike are processed in a group at once. This processing is done when an emitted spike is selected for processing, i.e., when the spike is propagated. This may not necessarily be the same moment as when the spike was emitted due to asynchrony. Because of these assumptions, analyzing the spike propagation order gives the same insights as analyzing the execution order of K_t .

Unlike the layered approach, with event-driven state updates neurons can theoretically fire more than once at the same time t . We prevent this by inducing a neuron to enter a refractory state for the remainder of time t . In this state, the neuron keeps its membrane potential at 0. This makes the model causally simpler, more tractable, and more "economic" when energy consumption is coupled to spike communication. These aspects also give an explicit retrospectively justification for the neurophysically observed refractoriness [3].

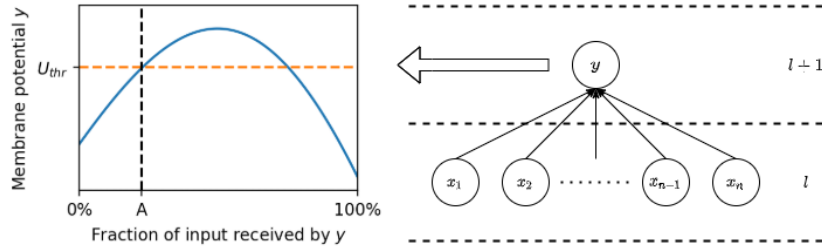


Figure 1: With network asynchrony, currents from neurons x_i in layer l may come to neuron y in layer $l+1$ at any time in any order. It may spike before all inputs have been received in a discrete timestep. Illustrated is the exceedance of the firing threshold at point A . All inputs, and thus information after A is missed, i.e., the spiking decision is made based on partial information. In this example, if layer synchronization is enforced, neuron y would wait for 100% of the input and will not spike.

The concept of time We apply input framing in discrete timesteps as typically done for inputs from a DVS sensor. The *timestep size* refers to the duration within which all input spikes are collected into a single matrix (also called frame), before being propagated throughout the network collectively in what is termed a *forward pass*. This input framing process precedes any network activity and follows the completion of all activity from the last forward pass. The timestamps of input spikes are rounded down to the nearest multiple of the timestep size.

The timestamps on the input spikes provide a meaningful measure of time. Upon arrival, they initiate network activity, making all new spikes contingent on their timing. Thus, they serve as the markers for the progression of time in timesteps, while the order of spike propagation through the network establishes another concept of “time” within a forward pass (or “micro-time” between timesteps).

3.1.2 Vectorized network asynchrony

The event-driven (neuron state) update rules for network asynchrony as introduced in the previous section can be vectorized by selecting multiple spikes for processing at the same time. This allows us to consider the entire spectrum of possibilities between full layer synchronization at one extreme, and “complete” asynchrony at the other extreme, where each spike event is processed entirely independently of all others. Additionally, vectorization makes acceleration possible by exploiting the parallelization features and vector pipelines of accelerators, where these models execute, leading to pragmatic simulation of network asynchrony.

During the simulation, the states of all the $N = \sum_{l=1}^L N^{(l)}$ neurons in the network are stored in vectors. The vector $\mathbf{x} \in \mathbb{R}^N$ tracks the computed input currents for the neurons, $\mathbf{u} \in \mathbb{R}^N$ the membrane potential of the neurons, $\mathbf{s} \in \mathbb{N}^N$ the emitted spikes queue, and $\mathbf{c} \in \mathbb{N}^N$ which neurons have spiked in the current forward pass. For any of those vectors, the indices from $\sum_{k=1}^{l-1} N^{(k)}$ to $\sum_{k=1}^l N^{(k)}$ represent the values for the neurons in layer l , for $1 \leq l \leq L$ where $N^{(0)} = 0$.

Algorithm 1 outlines the processing during a forward pass (propagation of the spikes of an input frame through the network). Before starting, the input spikes from time t_0 to t_1 are grouped, resulting in an input vector $\mathbf{s}_{\text{in}} \in \mathbb{N}^{N_{\text{in}}}$ where N_{in} is the number of input features. Then, the input spikes are passed as one single batch, triggering a forward pass. Each *forward pass* consists of *forward steps* (the code within

the while loop), which update the state of the neurons based on the spikes selected for propagation. A complete list of parameters can be found in section A.5.

Algorithm 1 Vectorized network asynchrony forward pass

Input: input spikes $\mathbf{s}_{\text{in}} \in \mathbb{N}^{N_{\text{in}}}$, previous forward pass time $t_0 \in \mathbb{R}$, current forward pass time $t_1 \in \mathbb{R}$, neuron state $\mathbf{u} \in \mathbb{R}^N$ at time t_0 , forward group size $F \in \mathbb{N}_{>0}$

Output: spike count $\mathbf{c} \in \mathbb{N}^N$

```

 $\Delta t \leftarrow t_1 - t_0$ 
 $\mathbf{u} \leftarrow \text{NeuronDecay}(\mathbf{u}, \Delta t)$ 
 $\mathbf{x} \leftarrow \text{InputLayerForward}(\mathbf{s}_{\text{in}})$ 
 $\mathbf{s} \leftarrow \mathbf{0}^N$  ▷ Vector with zeros of length  $N$ 
 $\mathbf{c} \leftarrow \mathbf{0}^N$ 
while ( $\text{Sum}(\mathbf{x}) \neq 0$  or  $\text{Sum}(\mathbf{s}) \neq 0$ ) and  $\neg \text{EarlyStop}(\mathbf{s})$  do
     $\mathbf{s}_{\text{new}}, \mathbf{u} \leftarrow \text{NeuronForward}(\mathbf{x}, \mathbf{u})$ 
     $\mathbf{s} \leftarrow \mathbf{s} + \mathbf{s}_{\text{new}}$  ▷ Enqueue new spikes
     $\mathbf{c} \leftarrow \mathbf{c} + \mathbf{s}_{\text{new}}$  ▷ Update spike count
     $\mathbf{s}_{\text{selected}} \leftarrow \text{SelectSpikes}(\mathbf{s}, F)$ 
     $\mathbf{s} \leftarrow \mathbf{s} - \mathbf{s}_{\text{selected}}$  ▷ Dequeue selected spikes
     $\mathbf{x} \leftarrow \text{NetworkLayersForward}(\mathbf{s}_{\text{selected}})$ 
end while

```

The forward pass always ends when all spike activations have been processed, a stop condition referred to as "On spiking done". Additionally, EarlyStop is used to interrupt a forward pass if any neuron in the output layer has spiked zero, one, or more (default is one) forward steps ago. This is termed the "On output" stop condition.

The SelectSpikes function defines how to select a subset of the emitted spikes for propagation. The function selects F spikes at a time, or less if there are less than F remaining spikes ready to be propagated. The method of spike selection is determined by a scheduling policy. For the experiments, two policies are considered. The first, Random Scheduling (RS), randomly picks spikes from the entire network. The second, Momentum Scheduling (MS), prioritizes spikes from neurons based on their membrane potential upon exceeding their threshold.

The neuron model-specific (LIF) behavior is expressed in the NeuronDecay and NeuronForward functions. This entails the computations for state updates (see section 3.1) for all neurons in the network (NeuronDecay) or for only those neurons receiving input currents in the forward step (NeuronForward), with added restriction that spiking is only allowed once per forward pass.

The network architecture is defined by the InputLayerForward and NetworkLayersForward functions. These functions compute the values of synaptic currents from spikes. For a network with only fully-connected layers, this follows from equation 3.

Imitating neuromorphic accelerator hardware Neuromorphic processors come in various architectures, but most of them have a template architecture that involves interconnecting many tiny processing cores with each other. This design enables a scalable architecture that supports fully distributed memory and compute systems. In this template, each processing core has its own small synchronous domain, but the cores are asynchronous among each other. For instance, the architectures of Loihi [10], SENECA [62], SpiNNaker [39], Speck [6], TrueNorth [1], POETS [50] and μ Brian [53] all follow this template. Our simulator imitates the behavior of a generalized neuromorphic processor by simulating the asynchronous interactions of several tiny synchronous domains and can be further customized to reproduce more intrinsic behavior of many of those processors (see table 4).

3.2 Training asynchronous SNNs

We use backpropagation to estimate the gradients of a loss function with respect to the weights. If multiple forward passes are needed, such as for sequential or temporal data, then Backpropagation Through Time (BPTT) can be used for training. Given that spike trains are temporal data as well, BPTT also applies to SNNs, and by extension, to the research presented here.

To address the issue of the non-differentiability of the threshold function, the surrogate gradient method is used [64]. An arctan function [13], (see section A.3 for details) provides a continuous and smooth approximation of the threshold function.

Class prediction is based on softmaxed spike counts over time, as described in section A.4. The loss is minimized using the Adam optimizer, with $\beta_1 = 0.9$ and $\beta_2 = 0.999$.

3.2.1 Unlayered backpropagation

Training of SNNs with per-layer synchronization is by now straightforward using backpropagation [9] so long as the forward processing is differentiable. We refer to this as "layered backpropagation".

The vectorized network asynchronous processing approach is differentiable as well, and can be used with backpropagation. We refer to this as "unlayered backpropagation". Combined with BPTT unrolling, this method implies a two level unrolling. In the outer level, unrolling is based on discretization of time in timesteps (when new inputs are provided); within the inner level, unrolling is based on the F -grouping of spikes, given a scheduling policy, and the activity of neurons up-until the output is read. For a single *backward pass*, which can be used in BPTT in a similar way as the layered backpropagation equivalent, it is given that:

$$\frac{\partial L_t}{\partial W} = \frac{\partial L_t}{\partial c_t} \sum_{i=1}^{N_t} \left(\frac{\partial c_t}{\partial s_i} \frac{\partial s_i}{\partial W} \right) \quad (1)$$

where t is the time(step) of the *forward pass*, W can be a weight on any of the synapses, L_t is the loss, c_t is the spike count at the end of the forward pass, and s_i are the spikes in the queue at the end of the forward step i , with N_t *forward steps* in total within the forward pass (referring to concept of (micro)-time in 3.1.1). The number of steps scales linearly with the number of spikes processed in the forward pass. It is important to understand that due to asynchronous processing the number of spikes processed until the evaluation of the loss function may be (well) less than the total number of spikes emitted. Since for every forward step, the computations are repeated, the time complexity scales linearly with the number of forward steps: $O(N_t)$. The same applies to the space complexity.

During the backward pass, the spikes which are not selected can skip the computation f for that step:

$$\frac{\partial s_i}{\partial W} = \frac{\partial f(s_{i-1;\text{selected}}, u_{i-1}, x_t, W)}{\partial W} + \frac{\partial s_{i-1;\text{not selected}}}{\partial W} \quad (2)$$

Skip connections have been researched in deep ANNs and identified as a major contributor to the stability of the training process [38]. This may apply to the skip in unlayered backpropagation as well. To what extent this is the case is not explored in this work.

3.2.2 Regularization techniques

During training, we use regularization to prevent overfitting and/or enhance model generalization. These techniques are not used during inference.

Input spike dropout. Randomly omits input spikes with a given probability. The decision to drop each spike is independent according to a Bernoulli distribution.

Weight regularization. Adds weight decay to the loss function: $L_{\lambda_W}(\mathbf{W}) = L(\mathbf{W}) + \lambda_W \|\mathbf{W}\|_2^2$ where λ_W is the regularization coefficient, L is the loss given the weights, and \mathbf{W} are all the weights.

Refractory dropout. With some probability, do not apply the refractory effect, allowing a neuron to fire again within the same forward pass.

Momentum noise. When using momentum scheduling, noise sampled from $U(0, 1)$ and multiplied by some constant λ_{MS} is added to the recorded membrane potential while selecting spikes.

4 Results

4.1 Experimental setup

We experimented with trained SNN models for asynchronous execution in three common benchmarking datasets: N-MNIST [37], SHD [8], and DVS gesture [2]. Each of them has different structure. N-MNIST has purely spatial structure, SHD purely temporal, and DVS gesture combines both spatial and temporal (i.e. input framing in DVS gesture is done such that an entire gesture motion and contour is not revealed within a single frame). More details on the datasets, can be found in section A.6.1. Table 1, summarizes the parameterization of the experiments and the reported results. The network architecture and hyperparameters are given in table 5. State-of-the art performance for these tasks can be achieved with reasonably shallow and wide models. We chose however to train narrow, but deeper network

architectures so that the effects of absence of layer synchronization can be revealed in the comparison (our aim is not to compete the state-of-the-art). In section A.7, details on how the forward group size, refractory dropout, and momentum noise during training affect accuracy are provided.

Table 1: Parameterization of experiments and results.

Parameterization	Description
Training method	Training with layered backpropagation is marked as "Layered" and with unlayered backpropagation as "Unlayered [scheduling strategy]".
Inference method	Inference with layer synchronization is marked as "Layered" and with network asynchrony as "Async [scheduling strategy]".
Scheduling strategy	How to select spikes from the queue. Can be random ("RS"), or based on the membrane potential just before spiking ("MS").
Forward group size F	Number of spikes to select for processing at the same time. Default is 8, both during training and inference.
Stop condition	Forward pass terminates: either when all network activity drains ("On spiking done") or one forward step after the first spike is emitted by the output layer ("On output"). The default is "On spiking done" during training and "On output" during inference.

4.2 Network asynchrony increases neuron reactivity

As observed in figure 2 (top row) during asynchronous inference, neurons are more reactive, i.e. a neuron can spike after integrating only a small number of incoming currents. With layer synchronization, this effect is averaged out as neurons are always required to consider all presynaptic currents (which are more likely to cancel each other out). For inference with $F = 8$, artifacts in the number of currents to spike can be observed, because each forward step propagates currents resulting from 8 spikes, causing neurons to integrate more currents than necessary for firing. Similar artifacts might also occur in neuromorphic chips equipped with fixed-width vector processing pipelines; making these observations insightful into the behavior of such hardware.

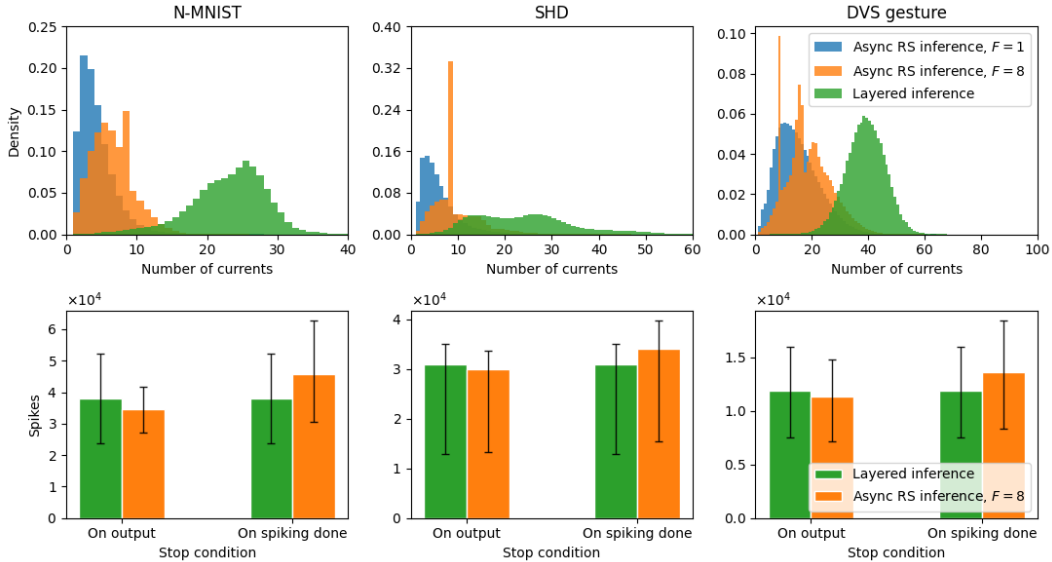


Figure 2: **(Top row)** Number of currents integrated by a neuron before spiking, recorded per neuron and per forward pass for all samples and neurons (excluding the neurons in the input layer). The Y-axis shows the relative frequency of the number of currents integrated before spiking. **(Bottom row)** Mean number of spikes per neuron during inference of all samples in the test. Error bars show the 25th and 75th percentiles. (Models in this figure were trained with layered backpropagation.)

Interestingly while one expects that more reactive neurons imply higher activation density, surprisingly

this is not the case for the models trained for asynchronous inference! In figure 2 (bottom row) we see that if we wait for the network to “drain” of spike activity the total number of spikes will indeed be higher, but if the forward pass terminates as soon as a decision is made, asynchronous models are consistently sparser. This is because asynchronous processing allows spike activity to freely flow through to the output and not be blocked at every layer for synchronization.

4.3 Unlayered backpropagation increases accuracy and sparsity

Network asynchrony negatively affects the performance of the models trained with layered backpropagation in all three datasets (table 2). This is likely in general the “Achilles’ heel” of neuromorphic AI today. However, we observe that the accuracy loss is remediated when using unlayered backpropagation, which also significantly increases sparsity (by about 2x). In fact, the accuracy of models trained and executed asynchronously is consistently superior under both scheduling policies (with momentum scheduling having consistently an edge). This result alone suffices to attest that neuromorphic AI is competitive and more energy efficient.

Figure 3 reveals another interesting result. It depicts how accuracy evolves as we allow more forward steps in the forward pass after the initial output during asynchronous inference. We see that because of the free flow of key information *depth-first*, models trained with unlayered backpropagation obtain the correct predictions as soon as the output layer gets stimulated. Activity that is likely triggered by “noise” in the input is integrated later on. Momentum scheduling is particularly good at exploiting this to boost accuracy.

Table 2: Accuracy and activation density results. More details about these metrics in section A.6.2.

Training	Inference	N-MNIST		SHD		DVS gesture	
		Acc.	Density	Acc.	Density	Acc.	Density
Layered	Layered	0.949	3.987	0.783	14.386	0.739	46.473
Layered	Async RS	0.625	3.652	0.750	13.905	0.701	44.140
Unlayered RS	Async RS	0.956	1.504	0.796	5.100	0.777	25.140
Unlayered MS	Async MS	0.963	1.476	0.816	6.224	0.856	26.686

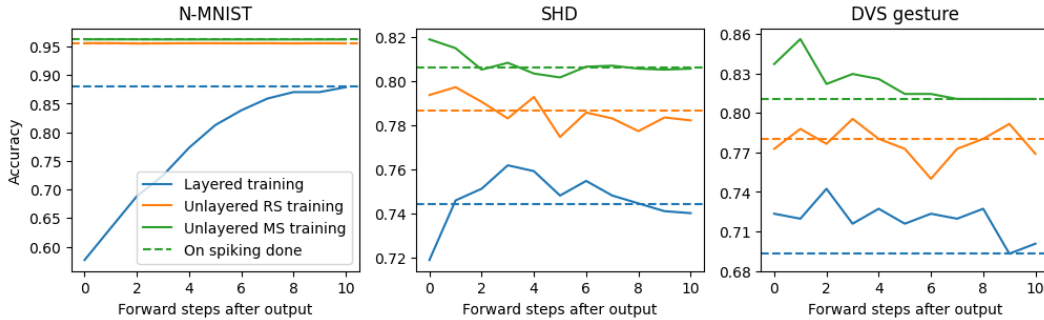


Figure 3: Accuracy as function of forward steps after the first spike in the output layer. Models trained with layer synchronization or random scheduling, are processed with random scheduling. Models trained with momentum scheduling, are processed with momentum scheduling. Given that $F = 8$, each extra forward step processes another 8 spikes, assuming enough spikes are available. Dashed lines show the accuracy after all spike activity has been “drained” out of the network.

4.4 Unlayered backpropagation decreases latency

The final and equally important result that we report is that under asynchronous network processing, models trained with unlayered backpropagation have significantly lower latency than those trained with layer synchronization. Assuming that, without parallel processing (worst case), latency is a function of the number of spikes processed until a decision is made, figure 4 shows a distribution of the inference latencies across the entire test-set. It should be clear by now that this is because “the important spikes” in these models quickly reach the output layer, uninhibited by layer synchronization.

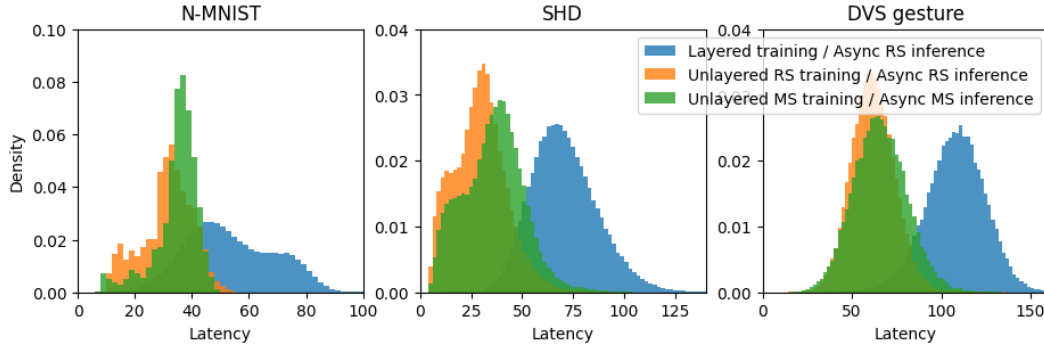


Figure 4: Latency per forward pass for all samples, in number of spikes until a decision in the output layer is reached. The Y-axis shows the relative frequency of recorded latencies.

4.5 Unlayered backpropagation is resource-intensive

The current implementation of unlayered backpropagation is costly when training with a smaller F and a larger dataset. When F is halved, the time and memory requirements approximately double, consistent with the linear time and space complexity discussed in section 3.2.1. The detailed results can be found in section A.8.

5 Discussion

We have introduced a variation of backpropagation training that does not assume per layer synchronization, and we use it to train models. Under asynchronous processing, these models exceed the performance of conventionally trained models and deliver the anticipated energy and latency efficiency from event-driven execution. Our findings show that unless we revise our training methods (taking into account asynchronous processing dynamics), and designs choices of neuromorphic accelerators (layer synchronization primitives considered harmful), SNNs and brain-inspired computing will likely fail to deliver either in performance or efficiency.

This study has merely scratched the surface. A key realization (that confirms neurobiology) is that trainable dynamics related to network asynchrony allow neurons (and models overall) to use partial input for decision making. The extent and generality of this effect on network architecture/structure, neuron models, and data types deserves further exploration. Our results also encourage a dynamics driven design space exploration for neuromorphic processors with regard to event processing scheduling and granularity of synchronization primitives (or lack thereof), which is almost absent today. The third exploration dimension is undoubtedly the resource efficiency and scalability of unlayered backpropagation (or analogous training framework) to facilitate very big models and datasets.

References

- [1] Filipp Akopyan, Jun Sawada, Andrew Cassidy, Rodrigo Alvarez-Icaza, John Arthur, Paul Merolla, Nabil Imam, Yutaka Nakamura, Pallab Datta, Gi-Joon Nam, et al. Truenorth: Design and tool flow of a 65 mw 1 million neuron programmable neurosynaptic chip. *IEEE transactions on computer-aided design of integrated circuits and systems*, 34(10):1537–1557, 2015.
- [2] Arnon Amir, Brian Taba, David Berg, Timothy Melano, Jeffrey McKinstry, Carmelo Di Nolfo, Tapan Nayak, Alexander Andreopoulos, Guillaume Garreau, Marcela Mendoza, et al. A low power, fully event-based gesture recognition system. In *Proceedings of the IEEE conference on computer vision and pattern recognition*, pages 7243–7252, 2017.
- [3] Michael Berry and Markus Meister. Refractoriness and neural precision. *Advances in neural information processing systems*, 10, 1997.
- [4] Lina Bonilla, Jacques Gautrais, Simon Thorpe, and Timothée Masquelier. Analyzing time-to-first-spike coding schemes: A theoretical approach. *Frontiers in Neuroscience*, 16:971937, 09 2022. doi: 10.3389/fnins.2022.971937.

- [5] Tom Brown, Benjamin Mann, Nick Ryder, Melanie Subbiah, Jared D Kaplan, Prafulla Dhariwal, Arvind Neelakantan, Pranav Shyam, Girish Sastry, Amanda Askell, et al. Language models are few-shot learners. *Advances in neural information processing systems*, 33:1877–1901, 2020.
- [6] Caterina Caccavella, Federico Paredes-Vallés, Marco Cannici, and Lyes Khacef. Low-power event-based face detection with asynchronous neuromorphic hardware. *arXiv preprint arXiv:2312.14261*, 2023.
- [7] Iulia-Maria Comşa, Krzysztof Potempa, Luca Versari, Thomas Fischbacher, Andrea Gesmundo, and Jyrki Alakuijala. Temporal coding in spiking neural networks with alpha synaptic function: Learning with backpropagation. *IEEE Transactions on Neural Networks and Learning Systems*, 33(10):5939–5952, 2022. doi: 10.1109/TNNLS.2021.3071976.
- [8] Benjamin Cramer, Yannik Stradmann, Johannes Schemmel, and Friedemann Zenke. The heidelberg spiking data sets for the systematic evaluation of spiking neural networks. *IEEE Transactions on Neural Networks and Learning Systems*, 33(7):2744–2757, 2020.
- [9] Manon Dampfhofer, Thomas Mesquida, Alexandre Valentian, and Lorena Anghel. Backpropagation-based learning techniques for deep spiking neural networks: A survey. *IEEE Transactions on Neural Networks and Learning Systems*, 2023.
- [10] Mike Davies, Narayan Srinivasa, Tsung-Han Lin, Gautham Chinya, Yongqiang Cao, Sri Harsha Choday, Georgios Dimou, Prasad Joshi, Nabil Imam, Shweta Jain, et al. Loihi: A neuromorphic manycore processor with on-chip learning. *Ieee Micro*, 38(1):82–99, 2018.
- [11] Peter U. Diehl, Daniel Neil, Jonathan Binas, Matthew Cook, Shih-Chii Liu, and Michael Pfeiffer. Fast-classifying, high-accuracy spiking deep networks through weight and threshold balancing. In *2015 International Joint Conference on Neural Networks (IJCNN)*, pages 1–8, 2015. doi: 10.1109/IJCNN.2015.7280696.
- [12] Rainer Engelken. Sparseprop: Efficient event-based simulation and training of sparse recurrent spiking neural networks. *Advances in Neural Information Processing Systems*, 36, 2024.
- [13] Wei Fang, Zhaofei Yu, Yanqi Chen, Timothée Masquelier, Tiejun Huang, and Yonghong Tian. Incorporating learnable membrane time constant to enhance learning of spiking neural networks. In *Proceedings of the IEEE/CVF international conference on computer vision*, pages 2661–2671, 2021.
- [14] S. B. Furber, F. Galluppi, S. Temple, and L. A. Plana. The spinnaker project. *Proceedings of the IEEE*, 102(5):652–665, 2014. doi: 10.1109/JPROC.2014.2304638.
- [15] Wenzhe Guo, Mohammed E. Fouda, Ahmed M. Eltawil, and Khaled Nabil Salama. Neural coding in spiking neural networks: A comparative study for robust neuromorphic systems. *Frontiers in Neuroscience*, 15, 2021. ISSN 1662-453X. doi: 10.3389/fnins.2021.638474. URL <https://www.frontiersin.org/journals/neuroscience/articles/10.3389/fnins.2021.638474>.
- [16] Yufei Guo, Yuanpei Chen, Liwen Zhang, YingLei Wang, Xiaode Liu, Xinyi Tong, Yuanyuan Ou, Xuhui Huang, and Zhe Ma. Reducing information loss for spiking neural networks. In *European Conference on Computer Vision*, pages 36–52. Springer, 2022.
- [17] Yufei Guo, Xuhui Huang, and Zhe Ma. Direct learning-based deep spiking neural networks: a review. *Frontiers in Neuroscience*, 17:1209795, 2023.
- [18] Weihua He, YuJie Wu, Lei Deng, Guoqi Li, Haoyu Wang, Yang Tian, Wei Ding, Wenhui Wang, and Yuan Xie. Comparing snns and rnns on neuromorphic vision datasets: Similarities and differences. *Neural Networks*, 132:108–120, 2020.
- [19] Dmitry Ivanov, Aleksandr Chezhegov, Mikhail Kiselev, Andrey Grunin, and Denis Larionov. Neuromorphic artificial intelligence systems. *Frontiers in Neuroscience*, 16:1513, 2022.
- [20] Laxmi R Iyer, Yansong Chua, and Haizhou Li. Is neuromorphic mnist neuromorphic? analyzing the discriminative power of neuromorphic datasets in the time domain. *Frontiers in neuroscience*, 15:608567, 2021.
- [21] Minseon Kang, Yongseok Lee, and Moonju Park. Energy efficiency of machine learning in embedded systems using neuromorphic hardware. *Electronics*, 9(7):1069, 2020.
- [22] Ziyang Kang, Lei Wang, Shasha Guo, Rui Gong, Shiming Li, Yu Deng, and Weixia Xu. Asie: An asynchronous snn inference engine for aer events processing. *ACM Journal on Emerging Technologies in Computing Systems (JETC)*, 16(4):1–22, 2020.

- [23] Saeed Reza Kheradpisheh and Timothée Masquelier. Temporal backpropagation for spiking neural networks with one spike per neuron. *International Journal of Neural Systems*, 30, 03 2020. doi: 10.1142/S0129065720500276.
- [24] Jaehyun Kim, Heesu Kim, Subin Huh, Jinho Lee, and Kiyoun Choi. Deep neural networks with weighted spikes. *Neurocomputing*, 311:373–386, 2018. ISSN 0925-2312. doi: <https://doi.org/10.1016/j.neucom.2018.05.087>. URL <https://www.sciencedirect.com/science/article/pii/S0925231218306726>.
- [25] Seijoon Kim, Seongsik Park, Byunggook Na, and Sungroh Yoon. Spiking-yolo: Spiking neural network for energy-efficient object detection. *Proceedings of the AAAI Conference on Artificial Intelligence*, 34: 11270–11277, 04 2020. doi: 10.1609/aaai.v34i07.6787.
- [26] Chit-Kwan Lin, Andreas Wild, Gautham N. Chinya, Yongqiang Cao, Mike Davies, Daniel M. Lavery, and Hong Wang. Programming spiking neural networks on intel’s loihi. *Computer*, 51(3):52–61, 2018. doi: 10.1109/MC.2018.157113521.
- [27] Yuhang Liu, Tingyu Liu, Yalun Hu, Wei Liao, Yannan Xing, Sadique Sheik, and Ning Qiao. Chip-in-loop snn proxy learning: a new method for efficient training of spiking neural networks. *Frontiers in Neuroscience*, 17:1323121, 2024.
- [28] Alexandra Sasha Luccioni, Sylvain Viguier, and Anne-Laure Ligozat. Estimating the carbon footprint of bloom, a 176b parameter language model. *Journal of Machine Learning Research*, 24(253):1–15, 2023.
- [29] William W Lytton and Michael L Hines. Independent variable time-step integration of individual neurons for network simulations. *Neural computation*, 17(4):903–921, 2005.
- [30] Wolfgang Maass. Networks of spiking neurons: the third generation of neural network models. *Neural networks*, 10(9):1659–1671, 1997.
- [31] Bruno Magalhães, Michael Hines, Thomas Sterling, and Felix Schürmann. Fully-asynchronous fully-implicit variable-order variable-timestep simulation of neural networks. In *Computational Science–ICCS 2020: 20th International Conference, Amsterdam, The Netherlands, June 3–5, 2020, Proceedings, Part V 20*, pages 94–108. Springer, 2020.
- [32] Bruno RC Magalhães, Thomas Sterling, Michael Hines, and Felix Schürmann. Fully-asynchronous cache-efficient simulation of detailed neural networks. In *Computational Science–ICCS 2019: 19th International Conference, Faro, Portugal, June 12–14, 2019, Proceedings, Part III 19*, pages 421–434. Springer, 2019.
- [33] Nico Messikommer, Daniel Gehrig, Antonio Loquercio, and Davide Scaramuzza. Event-based asynchronous sparse convolutional networks. In *Computer Vision–ECCV 2020: 16th European Conference, Glasgow, UK, August 23–28, 2020, Proceedings, Part VIII 16*, pages 415–431. Springer, 2020.
- [34] Lingfei Mo and Zhihan Tao. Evtsnn: Event-driven snn simulator optimized by population and pre-filtering. *Frontiers in Neuroscience*, 16:944262, 2022.
- [35] Massimo Monti, Manolis Sifalakis, Christian F. Tschudin, and Marco Luise. On hardware programmable network dynamics with a chemistry-inspired abstraction. *IEEE/ACM Transactions in Networking*, 25(4): 2054–2067, aug 2017. ISSN 1063-6692. doi: 10.1109/TNET.2017.2674690. URL <https://doi.org/10.1109/TNET.2017.2674690>.
- [36] Simon F Müller-Cleve, Vittorio Fra, Lyes Khacef, Alejandro Pequeño-Zurro, Daniel Klepatsch, Evelina Forno, Diego G Ivanovich, Shavika Rastogi, Gianvito Urgese, Friedemann Zenke, et al. Braille letter reading: A benchmark for spatio-temporal pattern recognition on neuromorphic hardware. *Frontiers in Neuroscience*, 16:951164, 2022.
- [37] Garrick Orchard, Ajinkya Jayawant, Gregory K Cohen, and Nitish Thakor. Converting static image datasets to spiking neuromorphic datasets using saccades. *Frontiers in neuroscience*, 9:437, 2015.
- [38] Emin Orhan and Xaq Pitkow. Skip connections eliminate singularities. In *International Conference on Learning Representations*, 2018.
- [39] Eustace Painkras, Luis A Plana, Jim Garside, Steve Temple, Francesco Galluppi, Cameron Patterson, David R Lester, Andrew D Brown, and Steve B Furber. Spinnaker: A 1-w 18-core system-on-chip for massively-parallel neural network simulation. *IEEE Journal of Solid-State Circuits*, 48(8):1943–1953, 2013.
- [40] Seongsik Park, Seijoon Kim, Hyeokjun Choe, and Sungroh Yoon. Fast and efficient information transmission with burst spikes in deep spiking neural networks. In *2019 56th ACM/IEEE Design Automation Conference (DAC)*, pages 1–6, 2019.

- [41] Seongsik Park, Seijoon Kim, Byunggook Na, and Sungroh Yoon. T2fsnn: Deep spiking neural networks with time-to-first-spike coding. *57th ACM/IEEE Design Automation Conference (DAC)*, pages 1–6, 2020. doi: 10.1109/DAC18072.2020.9218689.
- [42] Michael Pfeiffer and Thomas Pfeil. Deep learning with spiking neurons: Opportunities and challenges. *Frontiers in neuroscience*, 12:409662, 2018.
- [43] Guanchao Qiao, Ning Ning, Yue Zuo, Pujun Zhou, Mingliang Sun, Shaogang Hu, Qi Yu, and Yang Liu. Spatio-temporal fusion spiking neural network for frame-based and event-based camera sensor fusion. *IEEE Transactions on Emerging Topics in Computational Intelligence*, 2024.
- [44] Nitin Rathi, Indranil Chakraborty, Adarsh Kosta, Abhronil Sengupta, Aayush Ankit, Priyadarshini Panda, and Kaushik Roy. Exploring neuromorphic computing based on spiking neural networks: Algorithms to hardware. *ACM Computing Surveys*, 55(12):1–49, 2023.
- [45] Hongwei Ren, Yue Zhou, Haotian FU, Yulong Huang, Xiaopeng LIN, Jie Song, and Bojun Cheng. Spikepoint: An efficient point-based spiking neural network for event cameras action recognition. In *The Twelfth International Conference on Learning Representations*, 2024.
- [46] David P Rodgers. Improvements in multiprocessor system design. *ACM SIGARCH Computer Architecture News*, 13(3):225–231, 1985.
- [47] Bodo Rueckauer, Iulia-Alexandra Lungu, Yuhuang Hu, Michael Pfeiffer, and Shih-Chii Liu. Conversion of continuous-valued deep networks to efficient event-driven networks for image classification. *Frontiers in Neuroscience*, 11, 2017. doi: 10.3389/fnins.2017.00682. URL <https://www.frontiersin.org/journals/neuroscience/articles/10.3389/fnins.2017.00682>.
- [48] Sanaullah, Shamini Koravuna, Ulrich Rückert, and Thorsten Jungeblut. Exploring spiking neural networks: a comprehensive analysis of mathematical models and applications. *Frontiers in Computational Neuroscience*, 17:1215824, 2023.
- [49] Abhronil Sengupta, Yuting Ye, Robert Wang, Chiao Liu, and Kaushik Roy. Going deeper in spiking neural networks: Vgg and residual architectures. *Frontiers in neuroscience*, 13:95, 2019.
- [50] Mahyar Shahsavari, Jonathan Beaumont, David Thomas, and Andrew D. Brown. POETS: A Parallel Cluster Architecture for Spiking Neural Network. *International Journal of Machine Learning and Computing*, 11(4): 281–285, August 2021. ISSN 20103700. doi: 10.18178/ijmlc.2021.11.4.1048.
- [51] Mahyar Shahsavari, David Thomas, Marcel van Gerven, Andrew Brown, and Wayne Luk. Advancements in spiking neural network communication and synchronization techniques for event-driven neuromorphic systems. *Array*, 20:100323, 2023.
- [52] P Srivatsa, Kyle Timothy Ng Chu, Yaswanth Tavva, Jibin Wu, Malu Zhang, Haizhou Li, and Trevor E. Carlson. You only spike once: Improving energy-efficient neuromorphic inference to ann-level accuracy. *ArXiv*, abs/2006.09982, 2020. doi: 10.48550/arXiv.2006.09982.
- [53] Jan Stuijt, Manolis Sifalakis, Amirreza Yousefzadeh, and Federico Corradi. μ brain: An event-driven and fully synthesizable architecture for spiking neural networks. *Frontiers in neuroscience*, 15:664208, 2021.
- [54] Christian Szegedy, Sergey Ioffe, Vincent Vanhoucke, and Alexander Alemi. Inception-v4, inception-resnet and the impact of residual connections on learning. In *Proceedings of the AAAI conference on artificial intelligence*, volume 31, 2017.
- [55] Guangzhi Tang, Kanishkan Vadivel, Yingfu Xu, Refik Bilgic, Kevin Shidqi, Paul Detterer, Stefano Traferro, Mario Konijnenburg, Manolis Sifalakis, Gert-Jan van Schaik, and Amirreza Yousefzadeh. Seneca: building a fully digital neuromorphic processor, design trade-offs and challenges. *Frontiers in Neuroscience*, 17, 2023. ISSN 1662-453X. doi: 10.3389/fnins.2023.1187252.
- [56] Luke Taylor, Andrew King, and Nicol S Harper. Addressing the speed-accuracy simulation trade-off for adaptive spiking neurons. *Advances in Neural Information Processing Systems*, 36, 2024.
- [57] Ashish Vaswani, Noam Shazeer, Niki Parmar, Jakob Uszkoreit, Llion Jones, Aidan N Gomez, Łukasz Kaiser, and Illia Polosukhin. Attention is all you need. *Advances in neural information processing systems*, 30, 2017.
- [58] Athanasios Voulodimos, Nikolaos Doulamis, Anastasios Doulamis, and Eftychios Protopapadakis. Deep learning for computer vision: A brief review. *Computational intelligence and neuroscience*, 2018, 2018.
- [59] Timo C Wunderlich and Christian Pehle. Event-based backpropagation can compute exact gradients for spiking neural networks. *Scientific Reports*, 11(1):12829, 2021.

- [60] Leonid Yavits, Amir Morad, and Ran Ginosar. The effect of communication and synchronization on amdahl’s law in multicore systems. *Parallel Computing*, 40(1):1–16, 2014.
- [61] Amirreza Yousefzadeh, Mina A Khoei, Sahar Hosseini, Priscila Holanda, Sam Leroux, Orlando Moreira, Jonathan Tapon, Bart Dhoedt, Pieter Simoens, Teresa Serrano-Gotarredona, et al. Asynchronous spiking neurons, the natural key to exploit temporal sparsity. *IEEE Journal on Emerging and Selected Topics in Circuits and Systems*, 9(4):668–678, 2019.
- [62] Amirreza Yousefzadeh, Gert-Jan Van Schaik, Mohammad Tahghighi, Paul Detterer, Stefano Traferro, Martijn Hijdra, Jan Stuijt, Federico Corradi, Manolis Sifalakis, and Mario Konijnenburg. Seneca: Scalable energy-efficient neuromorphic computer architecture. In *2022 IEEE 4th International Conference on Artificial Intelligence Circuits and Systems (AICAS)*, pages 371–374. IEEE, 2022.
- [63] Semir Zeki. A massively asynchronous, parallel brain. *Philosophical Transactions of the Royal Society B: Biological Sciences*, 370(1668):20140174, 2015.
- [64] Friedemann Zenke and Tim P Vogels. The remarkable robustness of surrogate gradient learning for instilling complex function in spiking neural networks. *Neural computation*, 33(4):899–925, 2021.
- [65] Haiyan Zhao, Hanjie Chen, Fan Yang, Ninghao Liu, Huiqi Deng, Hengyi Cai, Shuaiqiang Wang, Dawei Yin, and Mengnan Du. Explainability for large language models: A survey. *ACM Transactions on Intelligent Systems and Technology*, 15(2):1–38, 2024.

A Appendix / supplemental material

A.1 Spiking neural networks

A.1.1 Incoming current

For every neuron layer, all the synaptic weights on its inbound connections are kept in a weight matrix $\mathbf{W}^{(l)} \in \mathbb{R}^{N^{(l)} \times N^{(l-1)}}$, where $N^{(0)}$ = number of input features N_{in} . Using these weight matrices, the total incoming current x for a neuron i in the next layer can be computed using:

$$x_i^{(l+1)}[t] = \sum_{j=1}^{N^{(l)}} W_{ij}^{(l+1)} s_j^{(l)}[t] \quad (3)$$

where $s_j^{(l)}[t]$ is 1 if neuron j in layer l has emitted a spike at time t , otherwise 0.

A.1.2 Membrane potential decay

The decay of the membrane potential is governed by a linear Ordinary Differential Equation (ODE). The analytical solution can be used to compute the decay:

$$u[t] = u[t - \Delta t] \cdot e^{-\frac{\Delta t}{\tau_m}} + x[t] \quad (4)$$

where τ_m is the membrane time constant and Δt the elapsed time.

A.1.3 Threshold function

$$\Theta(u) = \begin{cases} 1 & \text{if } u > U_{\text{thr}} \\ 0 & \text{otherwise} \end{cases} \quad (5)$$

where U_{thr} is the membrane potential threshold required for spiking.

A.2 Event-driven state update rule for LIF neuron

When an input current is received at time t by a neuron with a previous state $u[t_0]$ at some time $t_0 \leq t$, an atomic set of computations is executed. Start with computing the decayed membrane potential $u[t_-] = u[t_0] \cdot e^{-\frac{(t-t_0)}{\tau_m}}$, then update the membrane potential $u[t_+] = u[t_-] + x[t]$ with the input current $x[t]$, and finally set $u[t] = 0$ and emit a spike if $\Theta(u[t_+]) = 1$; otherwise $u[t] = u[t_+]$ without emitting a spike.

A.3 Arctan surrogate gradient

$$\Theta(u) = \frac{1}{\pi} \arctan(\pi u \frac{\alpha}{2}) \quad (6)$$

where α is a hyperparameter modifying the steepness of the function.

A.4 Class prediction

Class prediction involves first calculating the output rates as follows:

$$c_i = \sum_{t \in T} s[i, t] \quad (7)$$

where c_i is the spike count for class i , T are all the timesteps for which a forward pass occurred, and $s[i, t]$ is the output of the neuron representing class i in the output layer at the end of the forward pass at time t . These values are subsequently used as logits within a softmax function:

$$p_i = \frac{e^{c_i}}{\sum_{j=1}^{N_C} e^{c_j}} \quad (8)$$

where N_C is the total number of classes. The resulting probabilities are then used to compute the cross-entropy loss:

$$L = \sum_{i=1}^{N_C} y_i \log(p_i) \quad (9)$$

where $y \in \{0, 1\}^{N_C}$ is the target class in a one-hot encoded format.

A.5 Parameters for the simulator

Table 3: Overview of all current simulator parameters. If the text is *italic*, then the parameter was not used for the experiments in this paper.

Name	Value range	Description
Forward group size	$\mathbb{N}_{>0}$	3.1.2
Scheduling policy	RS/MS	3.1.2
Prioritize input	True/False	If input spikes are propagated before any spikes from inside the network.
Stop condition	On spiking done / On output	3.1.2
Forward steps after output	$\mathbb{N}_{\geq 0}$	3.1.2 (only for "On output" stop condition)
Refractory dropout	$[0.0, 1.0]$	3.2.2
Momentum noise	$\mathbb{R}_{\geq 0}$	3.1.2 (only for "MS" scheduling policy)
Membrane time constant	$\mathbb{R}_{>0}$	3.1
Input spike dropout	$[0.0, 1.0]$	3.2.2
<i>Network spike dropout</i>	$[0.0, 1.0]$	The same as input spike dropout, but for spikes from inside the network, applied per forward step.
Membrane potential threshold	$\mathbb{R}_{>0}$	3.1
Timestep size	$\mathbb{N}_{>0}$	3.1.1
<i>Synchronization threshold</i>	$\mathbb{N}_{\geq 0}$	Have neurons wait for a number of input currents (including barrier messages) before being allowed to fire. Can be set per neuron.
<i>Emit barrier messages</i>	True/False	Have neurons emit a barrier message if they have retrieved exactly the number of input currents to exceed the synchronization threshold, but not enough to exceed the membrane potential threshold.

Table 4: Simulator parameters for simulating neuromorphic processors

Synchronization type	Neuromorphic processors	Forward group size	Synchronization threshold [emit barrier messages]
Barrier-based / layer	Loihi [10], SENECA [62], POETS [50]	# neu/layer	# neu/layer [True]
Timer-based / core	SENECA [62], SpiNNaker [39], TrueNorth [1], POETS [50]	# neu/core	# neu/core [True]
Asynchronous	Speck [6], μ Brian [53]	# neu/layer	1 [False]

A.6 Details on the experimental setup

A.6.1 Datasets and network architectures

The Neuromorphic MNIST (N-MNIST) dataset captures the MNIST digits using a Dynamic Vision Sensor (DVS) camera. It presents minimal temporal structure [20]. It consists of 60000 training samples and 10000 test samples. Each sample spans approximately 300 ms, divided into three 100 ms camera sweeps over the same digit. Only the initial 100 ms segment of each sample is used in this study.

The Spiking Heidelberg Digits (SHD) dataset [8] is composed of auditory recordings with significant temporal structure. It consists of 8156 training samples and 2264 test samples. Each sample includes recordings of 20 spoken digits transformed into spike sequences using a cochlear model, capturing the rich dynamics of auditory processing. The 700 cochlear model output channels are downsampled to 350 channels.

The DVS gesture dataset [2] focuses on different hand and arm gestures recorded by a DVS camera. Like the SHD dataset, it has significant temporal structure. It focuses on 11 different hand and arm gestures recorded by a DVS camera. It consists of 1176 training samples and 288 test samples. The 128×128 input frame is downsampled to a 32×32 frame.

For all three datasets, input events are assigned a timestamp and an index. In the case of N-MNIST, the index corresponds to a position within a 34×34 pixel frame, with each pixel having a binary polarity value (either 1 or 0), leading to a total of $34 \times 34 \times 2 = 2312$ distinct input indices. For SHD, the index denotes one of the 350 output channels. For DVS gesture, the 128×128 input frame is downsampled to a 32×32 frame. Like N-MNIST, each pixel has a binary polarity value, so in total this gives $32 \times 32 \times 2 = 2048$ input indices.

Table 5: Network architecture and hyperparameters. The architecture is given as [input features] - [neurons in hidden layers \times number of hidden layers] - [neurons in output layer].

	N-MNIST	SHD	DVS gesture
Architecture	2312-[64 \times 3]-10	350-[128 \times 3]-20	2048-[128 \times 3]-11
Timestep size	10 ms	10 ms	20 ms
Batch size	256	32	32
Epochs	50	100	70
Learning rate	5e-4	7e-4	1e-4
Membrane potential threshold U_{thr}	0.3	0.3	0.3
Weight decay constant λ_W	1e-5	1e-4	1e-5
Membrane time constant τ_m	1 ms	100 ms	100 ms
Surrogate steepness constant α	2	10	10
Input spike dropout	0.25	0.2	0.2
Forward group size F	8	8	8
Refractory dropout	0.8	0.8	0.8
Momentum noise λ_{MS}	1e-6	0.1	0.1

A.6.2 Performance metrics

To evaluate accuracy, output rates c_i for each class i are first calculated as outlined in equation 7. The predicted class corresponds to the one with the highest output rate. Accuracy is then quantified as the ratio of correctly predicted outputs to the total number of samples.

Spike density is computed using:

$$\text{density} = \frac{1}{N_{\text{samples}} \cdot N_{\text{neurons}}} \sum_{i=1}^{N_{\text{samples}}} N_{\text{spikes}}[i] \quad (10)$$

where N_{samples} is the number of samples, N_{neurons} is the number of neurons in the hidden layers, and $N_{\text{spikes}}[i]$ is the total number of spikes during inference of the sample i .

A.7 Results on hyperparameters

Choosing a smaller F (i.e., with a more asynchronous system), may improve accuracy, particularly benefiting models with mechanisms that rely on network asynchrony such as momentum scheduling. However, reducing F also has its drawbacks. It significantly raises resource demands (discussed in section A.8), and there is a risk of reducing the effectiveness or even stalling the training process, as observed for SHD and DVS gesture.

Refractory dropout, can positively affect training outcomes. An explanation for this is that it increases the gradient flow by allowing more spiking activity. However, using full refractory dropout can also reduce performance, likely due to the inability to generalize to inference with refractoriness.

The momentum noise helps by introducing a slight stochastic element into the spike selection process, helping to avoid potential local minima that a purely deterministic selection method is prone to get stuck in. This seems to do little for N-MNIST, but for more complex datasets like SHD and DVS gesture it has a significant effect.

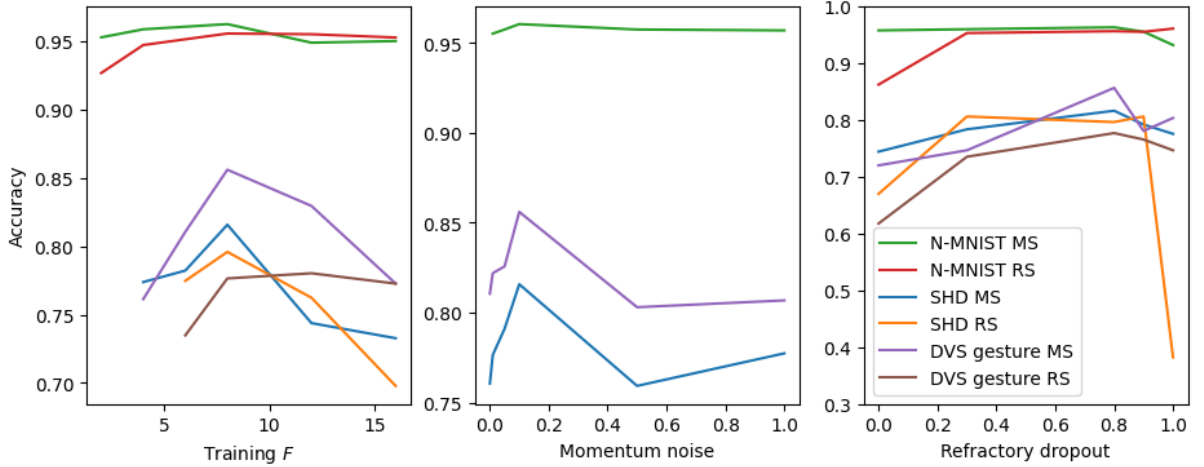


Figure 5: Results from inference with network asynchrony for different hyperparameters used during training. For SHD and DVS gesture with random scheduling, training F s smaller than 6 are not included due to the training failing to converge.

A.8 Results on resource usage

The increase in processing time is less pronounced for the N-MNIST and DVS gesture datasets compared to the SHD dataset. This discrepancy could be due to computational optimizations that apply specifically to the N-MNIST and DVS gesture datasets (both being vision-based datasets).

Table 6: Resource usage compared between layered and unlayered backpropagation during the second epoch of training on an NVIDIA Quadro RTX 5000.

Method	Time per epoch (s)	VRAM use (MB)
N-MNIST		
Layered	14	210
Unlayered RS, training $F = 16$	19	412
Unlayered RS, training $F = 8$	24	556
Unlayered RS, training $F = 4$	37	986
SHD		
Layered	38	214
Unlayered RS, training $F = 16$	118	2220
Unlayered RS, training $F = 8$	292	4844
Unlayered RS, training $F = 4$	681	10574
DVS gesture		
Layered	120	244
Unlayered RS, training $F = 16$	150	3802
Unlayered RS, training $F = 8$	177	6984
Unlayered RS, training $F = 4$	245	13914